Rotation of Coulomb Crystals in a Magnetized Inductively Coupled Complex Plasma

Felix M. H. Cheung, Nathan J. Prior, Leon W. Mitchell, Alexander A. Samarian, and Brian W. James

Abstract—**Under suitable conditions, micron-sized dust particles introduced into inductively coupled argon plasma form a stable microscopic crystal lattice, known as a Coulomb (or plasma) crystal. In the experiment described, an external axial magnetic field was applied to various configurations of Coulomb crystal, including small crystal lattices consisting of one to several particles, and large crystal lattices with many hundreds of particles. The crystals were observed to rotate collectively under the influence of the magnetic field. This paper describes the experimental procedures and the preliminary results of this investigation.**

Index Terms—**Complex plasma, crystal, dust, magnetic field, rotation.**

I. INTRODUCTION

COMPLEX PLASMA is low-temperature plasma consisting of electrons, ions, neutrals, and micrometer-sized particles of solid matter (dust particles). When micrometer-sized dust particles are released into plasma, they undergo collisions with the highly mobile electrons more frequently than with the slower heavier ions within the plasma. As a result, the dust particles accumulate thousands of electrons on their surface and become negatively charged. The interaction between the dust particles leads to the formation of a three-dimensional (3-D) lattice with an ordered structure similar to that of a crystal. Such dust crystals were first discovered in 1994 [1]–[4] and are now known as Coulomb or plasma crystals. These crystals are microscopic with an interparticle distance in the submillimeter region. When illuminated by a laser, the crystal structure is clearly visible to the naked eye. As dust crystals are physically realizable strongly coupled plasmas, and can be used as model systems for the investigation of phase changes and transport phenomena, they have attracted considerable attention [5]–[17].

At present, there is a shift of interests away from the problems of crystal formation to problems associated with the dynamical processes in the crystals. This includes investigation of the establishment and evolution of various microscopic collective motions excited by external influences, such as laser beams and biased electrodes [9], [12], [13], [17]–[24]. Until now, however, only a minimal number of experiments have been reported on the motion of dust crystal under the influence of an applied magnetic field. In the presence of an axial magnetic field, dust coulomb crystal rotation in a dc glow discharge was reported by Uchida *et al.* [25] and in a capacitive RF-discharge by Konopka *et al.* [26]. Depending on the discharge conditions, either rigid-body rotation or sheared rotation was observed. In the dc-discharge, the particles in the upper layers were observed to be rotating faster than the particles in the lower layers, corresponding to velocity shear in the vertical direction. A radial variation of angular velocity was reported in the RF-plasma case. The rotation was observed to be either right-handed or left-handed with respect to the direction of the axial magnetic field depending on the discharge parameters.

The reason such rotational behavior arises is still not properly understood. Nunomura *et al.* [27] proposed that the momentum transferred to the particles in the azimuthal direction by ion drag might be the cause of the crystal rotation. Whether the effect of the ion drag force is strong enough to initiate the rotation of the crystal is, however, still questionable. New experimental data for a variety of plasma conditions is needed in order to answer this question.

This paper describes an investigation of the rotation of small and large plasma crystals under the influence of an axial magnetic field in inductively coupled plasma. We define large dust crystals as those with more than 100 dust particles and small dust crystals as those with fewer than ten dust particles. To our knowledge, dust crystal rotation has not been reported previously in inductively coupled plasma.

II. APPARATUS

The experiments were carried out in a stainless steel cylindrical plasma chamber with an internal diameter of 19.5 cm and internal height of 19.5 cm. As shown in Fig. 1, there were four evenly spaced rectangular ports 5.5 cm wide and 10 cm high on end sides. Of the four, two adjacent ports had windows designed for observational purposes. The dust crystals were observed through one port using a Panasonic WV-BP554 video camera attached to an Olympus SZ-series microscope. A 110-Ls^{-1} turbo-molecular vacuum pump was connected to one port, and a magnetically coupled manipulated dust dispenser was mounted at another. A penning ionization gauge was used to measure the pressure near the pump inlet. Before each experiment, the chamber was evacuated to a pressure of approximately 10^{-6} torr. A high vacuum valve between the pump and
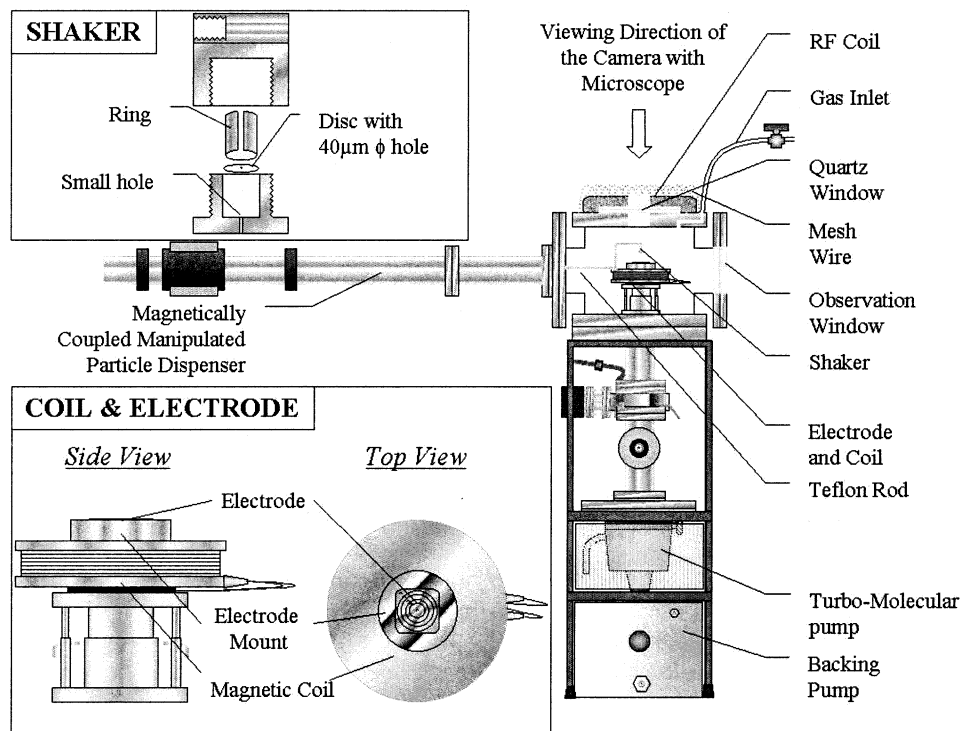
Fig. 1. Experimental apparatus used to produce the dust crystals. The inserts show the shaker used to disperse the micron-sized dust particles, the electrode, and the magnetic field coil.

the chamber allowed the chamber to be isolated from the pump during experiments.

The top of the chamber was sealed with a quartz plate, on top of which was a planar spiral RF coil consisting of eight turns copper tubing potted in araldite. A 6-cm-diameter hole in the center of the coil allowed observation of the dust crystal from above using another video camera attached to a microscope similar to the one on the side window.

The bottom of the chamber has a feed-through consisting of multiple tungsten pins through a ceramic disc, providing connections the electrode and the magnetic field coil below.

The argon gas, admitted into the vacuum chamber via an inlet port next to the RF coil, is used throughout the experiments. Power is supplied to the RF coil from a Hewlett Packard 3325A synthesizer/function generator via an A-300-RF power amplifier and matching network. The applied power is 50 W and the electron density and temperature measured by Langmuir probe are 10^9 cm^{-3} and 3 eV, respectively.

The melamine formaldehyde particles used in these experiments are spherical and monodisperse with a diameter of 6.21 ± 0.09 μm. They are stored in a shaker, connected by teflon rod to a magnetically coupled manipulation device which allows rotational and horizontal movement of the shaker. The shaker (see inset in Fig. 1) has a small 0.4-mm-diameter hole in its base, which screws off for refilling. A small copper disc with an approximately 40-μm-diameter hole is placed on top of the base before the particles are tipped in. The hole in the disc ensured that only small numbers of particles come out from the shaker. A gentle rotation of the magnetically coupled device causes the teflon rod to rotate, causing the shaker to sprinkle the particles

into the desired region. The shaker and rod are then pulled back to avoid obstructing the view of the dust crystal.

The dust crystal formed above the confining electrode is illuminated for observation by an 8-mW He-Ne laser. A half-cylindrical perspex lens in front of the laser causes the beam to diverge into a horizontal sheet. The motion of the dust crystals was observed through the microscope and via the video images from the cameras. The video output was passed through a sinc-function signal filter to increase image contrast, and the processed images were then recorded on videotapes at a frame rate of 50 fps, using a shutter speed of 0.008 s. The recorded images were captured with a National Instruments PCI-1408 IMAQ acquisition board. The particles were tracked using software that generated the x and y-coordinates of particles as a function of time.

The experiments involved creation of large, annular, and small plasma crystals, with different electrode arrangements used in each case. The electrodes were made from a conventional printed circuit board (PCB): Electrically isolated annular regions were created by etching or machining narrow circular breaks in the copper; electrical connections to the various regions were by pins through the insulating sheet. The electrodes were mounted on the magnetic field coil as shown in Fig. 1.

For the creation of large dust crystals, the electrode was made from a PCB disc of diameter 25 mm, in which a fine circle of diameter 9.8 mm was etched. To produce a confining potential well, a positive voltage of $+6$ V was applied to the central disc while the outer ring was grounded. The pressure in the chamber was 350 mtorr, and a 17.5 MHz, 400 mV p-p signal was applied to the RF coil. Dust crystals formed at most 5 mm above the electrode where the axial magnetic field was 130 G, as measured by a magnetometer.
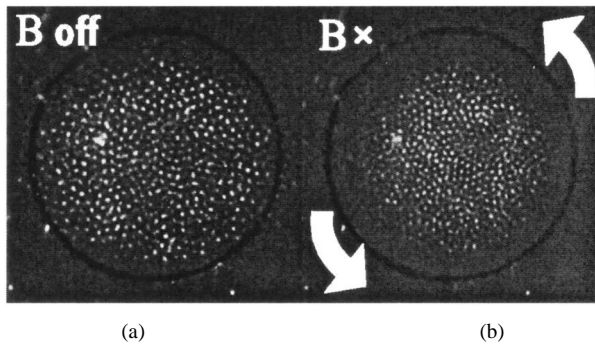
Fig. 2.   View from above of a large crystal (a) with and (b) without an axial magnetic field. The crystal rotates in the left-handed sense relative to the direction of the field.

For the production of annular dust crystals, narrow circles of diameter 7.1 and 12.3 mm were etched in a PCB disc of diameter 25.2 mm. A positive voltage of $+10$ V was applied to the intermediate annular region while the central an outer annular regions were grounded. The pressure was 250 mtorr of argon, and again an axial magnetic field of 130 G was used.

For small dust crystals consisting of one to several dust particles, the electrode consisted of a central disc of diameter 5 mm surrounded by three 2.4-mm-wide concentric annuli for use in future experiments with annular crystals (see insert in Fig. 1). To create a confining well, the central disc was powered with all other regions grounded. The voltage applied to the central disc was dependent on the crystal configuration desired, but typically $+10$ V was needed to form a crystal. The chamber was filled with 100 mtorr of argon. A different magnetic field coil produced fields of up to 31 G.

III. RESULTS AND ANALYSIS

Typical images of a large crystal are shown in Fig. 2. Approximately 1000 dust particles were dispersed into the plasma sheath, forming a crystal with two layers. The diameter of the crystal was about the same size as that of the electrode, which is about 11 mm in diameter. The top layer of the crystal consisted of a combination of hexagonal and pentagonal structures. The interparticle distance was 0.27 mm, and the crystal was levitated approximately 2 mm above the electrode.

Initially, when the magnetic field was off, the plasma crystal was stationary with small random fluctuations of the individual particles [see Fig. 2(a)]. When the magnetic field was switched on, the crystal rotated collectively in a left-handed sense [see Fig. 2(b)] with respect to the direction of the magnetic field. That is, for a vertically upwards field, the crystal rotated clockwise viewed from above. An increase in the magnetic field produced an increase in the angular velocity of the dust crystals. At a field of 130 G, the angular velocity was measured to be approximately one revolution per minute. No measurable difference in the angular velocity was observed at different radial distances from the center of the crystal, and there was no velocity shear between the layers of the crystal. Except for the random fluctuations, the integrity of the large plasma crystal was preserved during rotation.

An annular dust crystal, approximately 20 particles wide and with an interparticle separation of 0.22 mm, was formed above
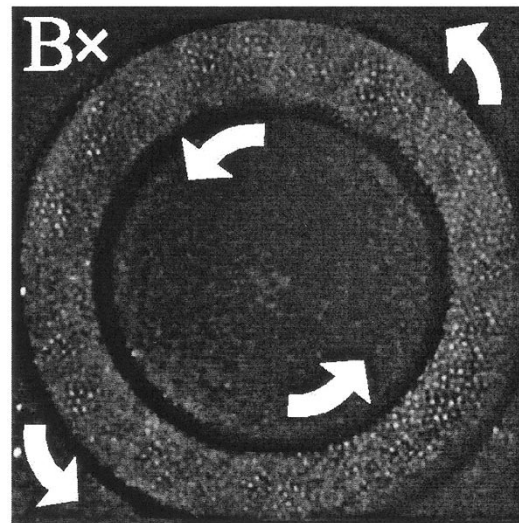

Fig. 3.   View from above of an annular crystal under the influence of an axial magnetic field. The crystal rotates in the left-handed sense relative to the direction of the field.
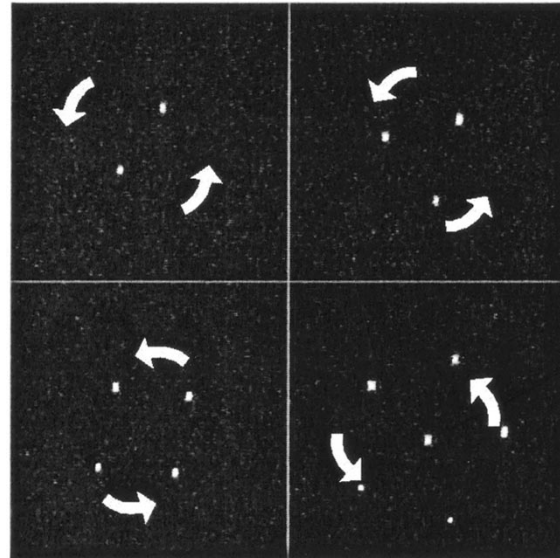

Fig. 4.   Images of planar-2, planar-3, planar-4, and planar-6 crystals.

the ring electrode (see Fig. 3). When the magnetic field was off, the particles in the annular dust crystal exhibited random fluctuations similar to those observed in large plasma crystal. When the magnetic field was at its maximum value, the ring crystal rotated collectively, again in the left-handed sense. The angular velocity was measured for fields of 130 G to be approximately 1 rpm. The particles within the inner region of the ring were moving at the same angular velocity as the particles in the outer region of the ring.

Small dust crystals of different structural configurations were formed. Fig. 4 shows images of structures consisting of two, three, four, and six particles in a plane. When the magnetic field was off, the small crystals exhibited small fluctuations but always remained in their most stable positions. When the magnetic field was switched on (unless otherwise specified, the maximum magnetic field of 31 G was applied), motion of the small crystals was observed.
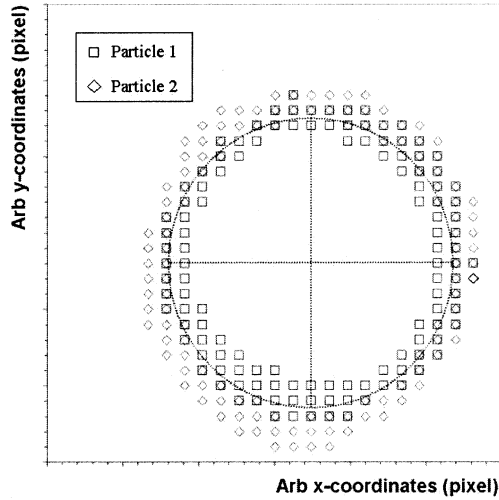
Fig. 5. Trajectories of the particles of a planar-2 crystal are circular when undergoing rotation.

Fig. 6. Angular position plotted as a function of time for the planar-2 crystal configuration.

For the one-dimensional (1-D) structural configurations consisting of one particle or of vertical strings of particles, no noticeable particle motion was observed in the vertical or horizontal directions. However, due to the axial symmetry of the particle configurations, the question of whether rotational motion was exhibited by the particles about their own axis remained undetermined. For the two-dimensional (2-D) structural configurations of planar-2, planar-3, planar-4, and planar-6 crystals, rotation in a left-handed sense similar to that in the large crystal systems was observed. Fig. 5 shows the angular locations, plotted as a function of time, for two particles which are diametrically opposite each other. Their trajectories during rotation are close to a circle. This is the first time such small crystal systems were observed experimentally to exhibit rotational behavior.

The angular positions of the individual particles in different planar configurations are shown as a function of time in Fig. 6. The results show that the angular positions of planar-3, planar-4, and planar-6 changed at a constant rate. On the other hand, the planar-2 crystal displayed quite different motion. First, the two particles remained diametrically opposite each other at all times during rotation. Second, the angular rotation of the two particles went through periodic pauses at a particular angle, which might be a result of the imperfect axial symmetry of the well.

The properties observed in the 3-D structural configurations were similar to those observed in 2-D. The trajectories of the individual particles of 2-on-1 (two particles in upper layer and one in lower), 3-on-1, 4-on-1, and 5-on-1 crystal structures, and of tetrahedral crystals are circular. The 3-on-1, 4-on-1, and 5-on-1 crystals rotated in the magnetic field with constant velocity, while the 2-on-1 crystal rotated with a periodic motion similar to that of the planar-2 crystal. Thus, it appeared more difficult to rotate planar-2 and the 2-on-1 crystals compared to the others.

The rotational motion of the 5-on-1 structure was investigated at different magnetic field strengths. The angular positions of the individual particles (except for the stationary particle at the center of the 5-on-1) were plotted as a function of time (see Fig. 7). The angular velocities of the 5-on-1 crystal at different magnetic field strength were determined from the slope of the
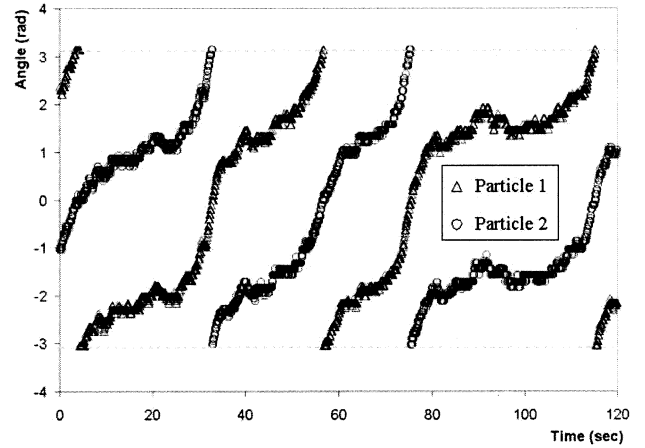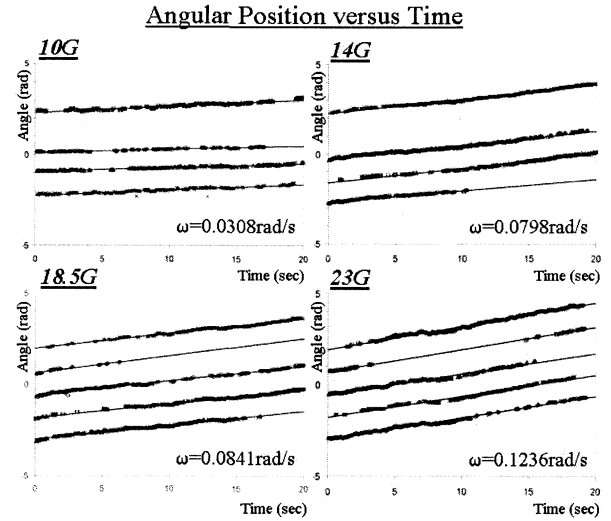

Fig. 7. Angular position plotted as a function of time for the 5-on-1 crystal configuration. The slope (i.e., the angular velocity) is constant for a particular value of magnetic field and increases as the magnetic field increases.

linear regression fits to the data. In Fig. 8, these values of angular velocity are plotted as a function of the magnetic field strength, showing that angular velocity increases linearly with magnetic field.

Consider the steady rotation of the plasma crystal in the horizontal plane. The rotation is governed by the balance of the radial electrostatic force F_r due to the confining electric field E_r, the azimuthal drive force F_d, the azimuthal friction force due to neutral-dust collisions F_f and the force due to the interaction between the particles F_{ip}. The interparticle interaction needs to be taken into account only in the case of spatially nonuniform systems. The driving force is the force that we attribute to the rotation of the plasma crystal. It could be the azimuthal component of the ion drag force, as was suggested by Konopka *et al.* [26] or another unidentified force with features we will analyze. The resulting equation of motion for the crystal, using cylindrical coordinates $\{r, \alpha\}$, where r is the radial distance from the center of rotation and α is the azimuthal angle, can be written as

$$\mathbf{e_r} m_d \omega^2 r = -\mathbf{e_r} F_r + \mathbf{e_r} F_{ip} + \mathbf{e_\alpha} F_d - \mathbf{e_\alpha} F_f \qquad (1)$$
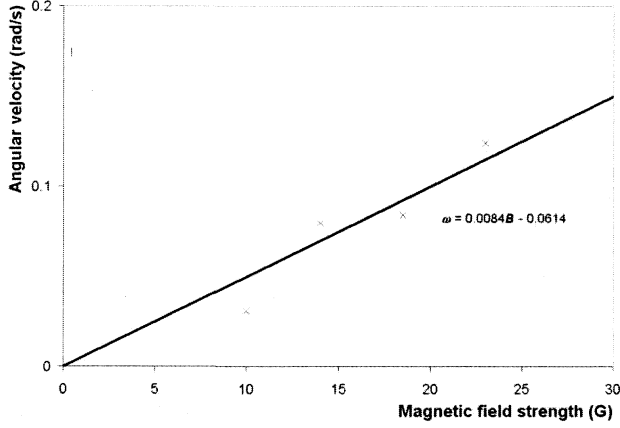
Fig. 8. Angular velocity plotted as a function of magnetic field strength for the 5-on-1 crystal configuration.

where m_d is the dust particle mass, ω is the angular velocity, and $\mathbf{e_r}$ and $\mathbf{e_\alpha}$ are the unit vectors in the radial and azimuthal directions, respectively. If we consider separately the forces acting in the azimuthal direction, for rigid body rotation the drive force must balance the friction force. We can estimate the friction force (under the assumption of complete accommodation of neutrals) using the expression [28]

$$F_f = -\delta(4/3)m_n n_n v_T \pi a^2 \omega \tag{2}$$

where $\delta \sim 1$ is a coefficient dependent on the type of scattering, m_n is the mass of the gas atom, $n_n = P/kT_n$ is the gas atom number density, P and T_n are the pressure and temperature of neutrals, respectively, $\nu_T = \sqrt{(8kT_n/\pi m_n)}$ is the average thermal speed of the atoms, a is the dust particle radius, and $\omega = \omega_d - \omega_n$ is the difference between the angular velocity of neutrals and dust particles. The value of angular velocity of neutrals ω_n can be roughly estimated by the following:

$$\omega_n = (\nu_{ni}/\nu_{nn})(u_\phi/r)$$

where ν_{ni} and ν_{nn} are the collisional frequency of ions and neutrals, respectively, $u_\phi = (\mu_0/p)^2 BE_C/[c(1+((\alpha_0/p))E_S)]$ is the azimuthal component of the ion drift velocity, p is the pressure, B is the magnetic field strength, E_S is the sheath electric field, E_C is the confining electric field, μ_0 is the zero field mobility, and α_0 is a constant for a particular gas [29]. The obtained value is 6×10^{-7} rads^{-1}. Moreover, we have experimental evidences that show there is no gas rotation. Thus, we can suggest that the gas is at rest and consider that $\omega = \omega_d$.

In this case, the magnitude of the driving force can be calculated from the friction force in the azimuthal direction. The values obtained are displayed in Table I. We can see that the magnitude of this force is significantly less than the forces acting in the vertical direction (for example gravitational force is 1.9 $\times 10^{-12}$ N). Using (2), along with the angular velocity dependence on magnetic field strength measured experimentally, we find that the driving force is linearly proportional to the magnetic field strength, $F_d \sim B$. Under the assumption that the crystal rotates due to the ion drag force [26], the angular velocity can be written as

$$\omega = \xi BE(r)/r \tag{3}$$

TABLE I
THE EXPERIMENTAL CONDITIONS, STRUCTURAL DIMENSION AND FEATURES, AND CALCULATED VALUES OF THE DRIVEN FORCE AND THE ION DRAG FORCE ARE TABULATED

	Big Crystal	Annular Crystal	5-on-1
Pressure	350mtorr	250mtorr	100mtorr
Electrode Voltage	+6V	+10V	+10V
Plasma Driving Voltage	400mV p-p	400mV p-p	400mV p-p
Plasma Driving Frequency	17.5MHz	17.5MHz	17.5MHz
Magnetic Field Strength	130G	130G	31G
Number of Particles	~1000	~1500	6
Diameter (B off)	10.77mm	6.14mm/11.88mm	1mm
Diameter (B on)	7.38mm	6.96mm/11.32mm	1mm
Angular velocity	0.1rad/sec	0.1rad/sec	0.1rad/sec
Driving Force	1.3E-15N	1.9E-15N	1.7E-16N
Ion Drag Force	5.6E-17N	3.9E-17N	9.6E-18N

where ξ is the constant determined by

$$\frac{\mu_0^2}{c} \frac{3}{4\delta} \frac{u_\Sigma}{v_{T_n}} \frac{1}{a^2 p^2} \frac{n_i}{n_n} \left(\frac{b_c^2 + 4b_{\pi/2}^2 \Gamma}{1 + (\alpha_0/p)E_S} \right)$$

Here, n_i is the ion density and u_Σ is the mean ion velocity. $b_c = a\sqrt{1 - (2eU/m_i u_\Sigma^2)}$ is the collection impact parameter where $U = -eZ/[4\pi\varepsilon_0 a(1 + a/\lambda_{De})]$ is the dust potential relative to the local plasma potential within the sheath, and λ_{De} is the electron Debye length; $b_{\pi/2} = e^2 Z/(4\pi\varepsilon_0 m_i u_\Sigma^2)$ is the orbit impact parameter whose asymptotic orbit angle is $\pi/2$; $\Gamma = (1/2)\ln[(\lambda_{De} + b_{\pi/2}^2)/(b_c^2 + b_{\pi/2}^2)]$ is the Coulomb logarithm integrated over the interval from b_c to λ_{De} [29].

In the case of a parabolic confining potential, the electric field is linearly proportional to r and the angular velocity should depend only on the magnetic field $\omega \sim B$. This fact agrees well with the measurements. To provide quantitative verification, we need to estimate the value of the ion drag force, which is given by the expression [30]

$$F_{id}^\phi = m_i n_i u_\Sigma \pi \left(b_c^2 + 4b_{\pi/2}^2 \Gamma \right) u_\phi \tag{4}$$

where m_i is the mass of the plasma ion.

The values obtained for the large annular and small plasma crystals are shown in Table I. It is easy to see that in comparison with the friction force, the ion drag force is smaller by about two orders of magnitude. This means that the assumption that the ion drag force as the driving force is not supported quantitatively.

Another possible mechanism for explaining the rotation is instability in the electric potential, which occurs due to a spatial gradient of dust charge [31]. This charge variation can be present in dusty plasma systems due to inhomogeneity of the bulk plasma surrounding the dust crystal, for example, due to gradients of temperature T_e (T_i) and density n_e (n_i) of electrons (ions) in the plasma. Apparently, the magnetic field modifies the radial profile of the electron and ion density. This effect is presumably due to the magnetization of the electrons. In fact, for our experimental conditions, the ratio of the electron gyrofrequency to the frequency of the electron-neutral collisions exceeds unity, and is ~1.5; for the ions, this ratio is less than 0.01. The change of radial distribution of $n_e(n_i)$ can lead to an increase in the dust charge spatial gradient $\beta_r = \partial Z(r)/\partial r$. If there is a preferred direction in our system, then this may be the reason for the plasma crystal rotation. It should be mentioned
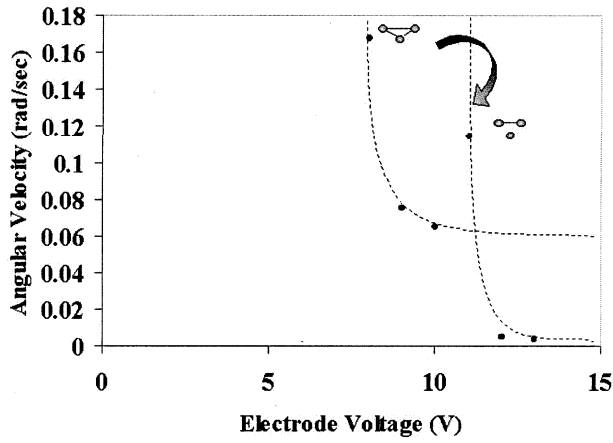
Fig. 9. Angular velocity of a planar-3 crystal decreases as the confining electrode voltage increases. The effect continues until the dust crystal changes its structure to compensate for the high electrode voltage. The angular velocity changes to a higher value and then decreases again with increasing electrode voltage.

that the rotational behavior of planar-2 and 2-on-1 crystal shows the existence of a preferred direction in our system. The angular velocity of rotation can be estimated from [32]

$$\omega = F_{\text{non}}\beta_r / 2m_d Z \nu_{fr} \qquad (5)$$

where F_{non} is a nonelectric force, Z is the dust particle charge, and ν_{fr} is the collisional frequency.

For the nonelectric force, different forces can be considered. For example, the thermophoretic force

$$F_{th}(r) = -(32/15)\sqrt{\frac{\pi m_n}{8T}}\, a^2 \chi \frac{\partial T}{\partial r}$$

where χ is the heat conductivity. In this case, estimates of the value of the charge gradient $\beta_r / \langle Z \rangle$ which would be sufficient to drive the rotation can be found by substituting the expression for F_{th} into (5)

$$\beta_r / \langle Z \rangle\,[\text{cm}^{-1}] = 2.8\omega\,[\text{rads}^{-1}]P\,[\text{torr}]/(\partial T/\partial r)\,[\text{K}\cdot cm^{-1}]. \qquad (6)$$

The temperature gradient in the sheath is about 0.5 Kcm^{-1}, therefore, $\beta_r / \langle Z \rangle = 0.2, 0.14$, and 0.06 cm^{-1}, respectively, for large, annular, and small crystals. These are quite reasonable values for inductively coupled plasmas.

Another interesting observation illustrating the influence of the magnetic field on $n_e(n_i)$ is the decrease in the size of the plasma crystal after the application of the field [see Fig. 2(a) and (b)]. The diameters of various crystals, with and without magnetic field, are shown in Table I. This suggests a change in the confining potential, specifically an increase in the radial electric field when a magnetic field is applied.

We can also change the radial electric field by varying the voltage applied to the confining electrode. In terms of the ion drag model, we would expect an increase in angular velocity with increasing electrode voltage. The experiment, however, shows the opposite. In Fig. 9, the angular velocity is shown as a function of electrode voltage for the planar-3

crystal and a magnetic field strength of 31 G. It can be seen that when the magnitude of the electrode voltage is sufficiently high, a structure transition occurs, with the planar-3 crystal transforming to a 2-on-1 crystal. The angular velocity increases immediately for the 2-on-1 structure, but then decreases again as the electrode voltage is increased.

IV. CONCLUSION

It has been demonstrated by experiment that under the influence of an axial magnetic field, large, annular, and small plasma crystals produced in inductively coupled RF plasma undergo left-handed rotation. An increase in the magnetic field strength produces an increase in the angular velocity of the crystal, and a reversal of the direction of the magnetic field produces a reversal in the direction of the sense of rotation. Neither radial variation in angular velocity nor velocity shear in the vertical direction was observed.

Planar-2 and 2-on-1 crystals exhibit periodic pausing in their rotation and these two crystal structures are more resistant to rotation initiated by the magnetic field. From the rotational motion of the 5-on-1 crystal, linear variation of angular velocity with magnetic field strength was demonstrated. Angular velocity decreased as the confining electrode voltage increased.

An attempt to attribute the rotation of plasma crystals to the action of the ion drag force gives only qualitative agreement with the experimental data, as the value of ion drag force is not large enough to explain the observed value of angular velocity. A possible explanation of the observed motion in terms of a change in the confining electric field requires further experimental investigation.

REFERENCES

[1] J. H. Chu and I. Lin, "Direct observation of coulomb crystals and liquids in strongly coupled rf dusty plasmas," *Phys. Rev. Lett.*, vol. 72, p. 4009, 1994.
[2] H. Thomas, G. E. Morfill, V. Demmel, J. Goree, B. Feuerbacher, and D. Möhlmann, "Plasma crystal: Coulomb crystallization in a dusty plasma," *Phys. Rev. Lett.*, vol. 73, p. 652, 1994.
[3] Y. Hayashi and K. Tachibana, "Observation of coulomb-crystal formation from carbon particles grown in a methane plasma," *Jpn. J. Appl. Phys.*, vol. 33, p. L804, 1994.
[4] A. Melzer, T. Trottenberg, and A. Piel, "Experimental determination of the charges on dust particles forming coulomb lattices," *Phys. Lett. A*, vol. 191, p. 301, 1994.
[5] A. Barkan, N. D'Angelo, and R. L. Merlino, "Laboratory observation of the dust-acoustic wave mode," *Phys. Plasmas*, vol. 2, p. 3563, 1995.
[6] G. Praburam and J. Goree, "Experimental observation of very low-frequency macroscopic modes in a dusty plasma," *Phys. Plasmas*, vol. 3, p. 1212, 1996.
[7] V. E. Fortov, A. P. Nefedov, O. F. Petrov, A. A. Samarian, and A. V. Chernyschev, "Emission properties and structural ordering of strongly coupled dust particles in a thermal plasma," *Phys. Lett. A*, vol. 219, p. 89, 1996.
[8] M. Zuzic, H. Thomas, and G. Morfill, "Wave propagation and damping in plasma crystals," *J. Vac. Sci. Technol. A*, vol. 14, p. 496, 1996.
[9] J. Pieper and J. Goree, "Dispersion of plasma dust acoustic waves in the strong-coupling regime," *Phys. Rev. Lett.*, vol. 77, p. 3137, 1996.
[10] A. Melzer, A. Homann, and A. Piel, "Experimental investigation of the melting transition of the plasma crystal," *Phys. Rev. E, Stat. Phys. Plasmas Fluids Relat. Interdiscip. Top.*, vol. 53, no. 3, p. 2757, 1996.
[11] V. E. Fortov, A. P. Nefedov, V. M. Torchinsky, V. I. Molotkov, O. F. Petrova, A. A. Samarian, A. M. Lipaev, and A. G. Khrapaka, "Crystalline structures of strongly coupled dusty plasmas in dc glow discharge strata," *Phys. Lett. A*, vol. 229, 1997.
[12] A. Homann, A. Melzer, R. Madani, and A. Piel, "Laser excited dust lattice waves," *Phys. Lett. A*, vol. 242, p. 173, 1998.

[13] R. L. Merlino, A. Barkan, C. Thompson, and N. D'Angelo, "Laboratory studies of waves and instabilities in dusty plasmas," *Phys. Plasmas*, vol. 5, p. 1607, 1998.

[14] Y. V. Gerasimov, A. P. Nefedov, V. A. Sinel'shchikov, and V. E. Fortov, "Formation of macroparticle structures in an RF induction discharge plasma," *Tech. Phys. Lett.*, vol. 24, p. 774, 1998.

[15] H. H. Hwang, E. R. Keiter, and M. J. Kushner, "Consequences of 3-dimensional physical and electromagnetic structures on dust particle trapping in high plasma density materials processing discharges," *J. Vac. Sci. Technol. A*, vol. 16, p. 2454, 1998.

[16] S. Nunomura, N. Ohno, and S. Takamura, "Confinement and structure of electrostatically coupled dust clouds in a direct current plasma-sheath," *Phys. Plasmas*, vol. 5, p. 3517, 1998.

[17] K. Takahashi, T. Oishi, K. Shimomai, Y. Hayashi, and S. Nishino, "Analyzes of attractive forces between particles in coulomb crystal of dusty plasmas by optical manipulations," *Phys. Rev. E, Stat. Phys. Plasmas Fluids Relat. Interdiscip. Top.*, vol. 58, no. 6, p. 7805, 1998.

[18] D. A. Law, W. H. Steel, B. M. Annaratone, and J. E. Allen, "Probe-induced particle circulation in a plasma crystal," *Phys. Rev. Lett.*, vol. 80, p. 4189, 1998.

[19] G. E. Morfill, H. M. Thomas, U. Konopka, H. Rothermel, M. Zuzic, A. Ivlev, and J. Goree, "Condensed plasmas under microgravity," *Phys. Rev. Lett.*, vol. 83, p. 1598, 1999.

[20] V. I. Molotkov, A. P. Nefedov, V. M. Torchinskii, V. E. Fortov, and A. G. Khrapak, "Dust acoustic waves in a dc glow-discharge plasma," *JETP*, vol. 89, p. 477, 1999.

[21] S. Nunomura, T. Misawa, N. Ohno, and S. Takamura, "Instability of dust particles in a coulomb crystal due to delayed charging," *Phys. Rev. Lett.*, vol. 83, p. 1970, 1999.

[22] Y. Wang, W. Juan, and I. Lin, "Self-organized oscillations of strongly coupled dust coulomb clusters in plasma traps," *Phys. Rev. E, Stat. Phys. Plasmas Fluids Relat. Interdiscip. Top.*, vol. 62, p. 5667, 2000.

[23] M. Klindworth, A. Melzer, and A. Piel, "Laser-excited intershell rotation of finite coulomb clusters in a dusty plasma," *Phys. Rev. B, Condens. Matter*, vol. 61, p. 8404, 2000.

[24] A. A. Samarian, A. V. Chernyshev, O. F. Petrov, A. P. Nefedov, and V. E. Fortov, "An analysis of acoustic oscillations in dust plasma structures," *JETP*, vol. 92, p. 454, 2001.

[25] G. Uchida, R. Ozaki, S. Iizuka, and N. Sato, "Dust vortex in a dc discharge plasma under a weak magnetic field," in *Proc. ICPP 25th EPS Conf. Controlled Fusion and Plasma Physics*, Praha, Czech Republic, Jun. 29–Jul. 3, 1998, ECA 22C, p. 2557.

[26] U. Konopka, D. Samsonov, A. V. Ivlev, J. Goree, V. Steinberg, and G. E. Morfill, "Rigid and differential plasma crystal rotation induced by magnetic fields," *Phys. Rev. E, Stat. Phys. Plasmas Fluids Relat. Interdiscip. Top.*, vol. 61, p. 1890, 2000.

[27] S. Nunomura, N. Ohno, and S. Takamura, "Effects if ion flow by $E \times B$ behavior in magnetized cylindrical electron cyclotron resonance plasmas," *Jpn. J. Appl. Phys.*, pt. 1, vol. 36, p. 877, 1997.

[28] P. S. Epstein, "On the resistance experienced by spheres in their motion through gases," *Phys. Rev.*, vol. 23, p. 710, 1924.

[29] L. S. Frost, "Effect of variable ionic mobility on ambipolar diffusion," *Phys. Rev.*, vol. 23, p. 710, 1924.

[30] M. S. Barnes, J. H. Keller, J. C. Forster, J. A. O'Neill, and D. K. Coultas, "Transport of dust particles in glow-discharge plasmas," *Phys. Rev. Lett.*, vol. 68, no. 3, p. 313, 1992.

[31] O. S. Vaulina, A. P. Nefedov, O. F. Petrov, and V. E. Fortov, "Instability of plasma–dust systems with a macroparticle charge gradient," *JETP*, vol. 91, p. 1147, 2000.

[32] A. Samarian, O. Vaulina, and B. W. James, "Formation of vertical and horizontal dust vortexes in an rf-dischargA," in *Phys. Scr.*, vol. T98, 2002, p. 123.

Felix M. H. Cheung received the B.Sc. (with honors) degree from the Flinders University of South Australia, Adelaide, Australia, in 1999. He is currently working toward the Ph.D. degree from the Complex Plasma Laboratory, the University of Sydney, Sydney, Australia.

He first started his research on complex (dusty) plasma in 1999, and he has been conducting research on the effect of external fields on complex dust crystals ever since.

Nathan J. Prior has performed undergraduate and postgraduate studies at Flinders University of South Australia, Adelaide, Australia, where he is currently working toward the Ph.D. degree while in close collaboration with the University of Sydney, Sydney, Australia.

In 1996, he built the dusty plasma apparatus at Flinders University. His research interests include oscillations and rotations of few particle structures. His theoretical investigations include forces between vertically aligned particles.

Leon W. Mitchell, photograph and biography not available at the time of publication.

Alexander A. Samarian received the Ph.D. degree in plasma physics and chemistry from the Institute for High Temperatures, Russian Academy of Science, Moscow, Russia, in 1997.

He was a Senior Research Scientist with the Institute of High Energy Densities (IHED), Moscow, until 2000, when he joined the School of Physics, University of Sydney, Sydney, Australia. Currently, he is a Principal Investigator with the Complex Plasma Laboratory, University of Sydney. During his tenure at IHED, he performed research of complex thermal plasmas and developed novel diagnostic methods for the measurement of complex plasma parameters, electrophysical and optical properties of strongly coupled plasmas and dusty plasma crystals. His recent research interests include theoretical and experimental investigations of dynamic phenomena in glow discharge complex plasmas, development of novel diagnostic tools, and later, the application of complex plasmas to the nanoprocessing.

Brian W. James received the Ph.D. degree from the University of Sydney, Sydney, Australia, in 1971.

His research interests include plasma diagnostics of both high-temperature magnetically confined plasmas and low-temperature processing plasmas. His interest in complex (dusty) plasma arose from a general interest in the behavior of sheaths in processing plasmas. He is currently an Associate Professor with the School of Physics, University of Sydney, and an Associate Dean (postgraduate research) with the University's Faculty of Science.